



DETECTION OF TROPOSPHERIC OZONE BY REMOTE SENSING FROM THE GROUND

YIBO JIANG,^a YUK L. YUNG,^{a†} and STANLEY P. SANDER^b

^aDivision of Geological and Planetary Sciences, California Institute of Technology, Pasadena, CA 91125 and ^bEarth and Space Sciences Division, Jet Propulsion Laboratory, California Institute of Technology, Pasadena, CA 91109, U.S.A.

(Received 18 July 1996)

Abstract—Due to larger multiple scattering effects in the troposphere compared to that in the stratosphere, the optical path of tropospheric ozone is markedly enhanced (as compared with that of stratospheric ozone) in the Huggins bands from 310 to 345 nm. Model study of the direct and diffuse solar fluxes on the ground shows differences between tropospheric and stratospheric ozone. The characteristic signature of tropospheric ozone enables us to distinguish a change in tropospheric ozone from that of stratospheric ozone. A simple retrieval algorithm is used to recover the tropospheric column ozone from simulated data. © 1997 Elsevier Science Ltd

1. INTRODUCTION

Tropospheric ozone plays a key role in regulating the chemical composition and climate of the troposphere.^{1,2} There is general agreement that tropospheric ozone has increased globally in recent decades,^{3,4} but the lack of reliable global measurements of tropospheric ozone sets a limit on our ability to predict the variations of this tropospheric chemical species.

Since the tropospheric column ozone is only about 10% of that in the stratosphere, the spectroscopic signal (e.g., in absorption measurements) from tropospheric ozone is usually overwhelmed by the contribution from the much larger stratospheric ozone layer. Therefore, the measurement of the tropospheric ozone by a remote sensing technique has always been a challenge. In this paper, we will investigate the possibility of detecting tropospheric ozone by measuring the atmospheric radiation in the Huggins bands in the range from 310 to 345 nm using an interferometric spectrometer.⁵ In the following we shall assume that the u.v. instrument will be used to make observations on the ground.

O₃ and SO₂ are the principal absorbing species in the spectral region of the Huggins bands in the Earth's atmosphere. Since the concentration of SO₂ (on the order of 1 ppbv at low altitudes) is much less than that of O₃, and the absorption cross sections are about the same, the absorption of solar radiation by SO₂ can be neglected in this study, except during or immediately after volcanic eruptions. The Huggins bands consist of a series of characteristic alternating absorption minima and maxima as shown in Fig. 1. The temperature-dependent ozone absorption cross section data (Fig. 1) in the Huggins bands is from Malicet et al⁶ with resolution of 0.01 nm at 5 temperatures (218, 228, 243, 273 and 295 K). As is clearly demonstrated in this figure, the cross section of ozone in the Huggins bands is strongly dependent on the temperature. In particular, the temperature dependence of the cross section appears to be different for the maxima and the minima, with the minima being more strongly dependent on the temperature.

The underlying principle of the proposed technique is very simple and is based on three facts:

1. u.v. radiation reaches the surface of the Earth by two pathways: direct propagation from the Sun, and diffuse radiation that has undergone multiple scattering in the atmosphere;

†To whom all correspondence should be addressed.

2. most photons that are absorbed or scattered in the stratosphere have undergone a single scattering process. The photons that are absorbed or scattered in the troposphere have gone through multiple scattering;
3. the ratio of the diffuse radiation to the direct solar radiation provides a useful measure of the multiply to singly scattered photons.

As we shall show later, we can discriminate between tropospheric and stratospheric ozone by making suitable measurements of the diffuse to direct radiation ratio (to be defined later).

2. THE RADIATIVE MODEL

To investigate quantitatively the radiative properties of atmospheric ozone in the Huggins bands, we used a radiative transfer model consisting of 80 vertical layers from 0 to 80 km with vertical resolution 1 km. This model computes accurately multiple scattering using a method described by Michelangeli et al.⁷ and it includes the effects of absorption, Rayleigh and aerosol scattering without polarization.

The vertical profiles of temperature, number density and ozone concentration of the 1976 U.S. Standard Atmosphere (see Fig. 2) are used in the model. The Standard Atmosphere does not have ozone concentration at the ground level. We set it equal to the value of the nearest level (2 km) $6.80 \times 10^{11} \text{ cm}^{-3}$ or 26.7 ppmv. We define the tropopause based on the temperature inversion at 12 km. From this definition, the total column ozone density in the atmosphere is 347.22 DU, with 310.34 DU in the stratosphere and 36.88 DU in the troposphere. The aerosol vertical profile (Fig. 2) and the size distribution are taken from Demerjian et al.⁸ The maximum radius of this distribution and the complex refractive index of the particles are $0.07 \mu\text{m}$ and $1.5-0.1i$, respectively. The Earth's surface albedo is set to 0.1.⁹

Figure 3 shows the total optical depth of this standard atmosphere in the Huggins bands. Rayleigh and aerosol scattering optical depths are nearly constant in the bands. At wavelengths

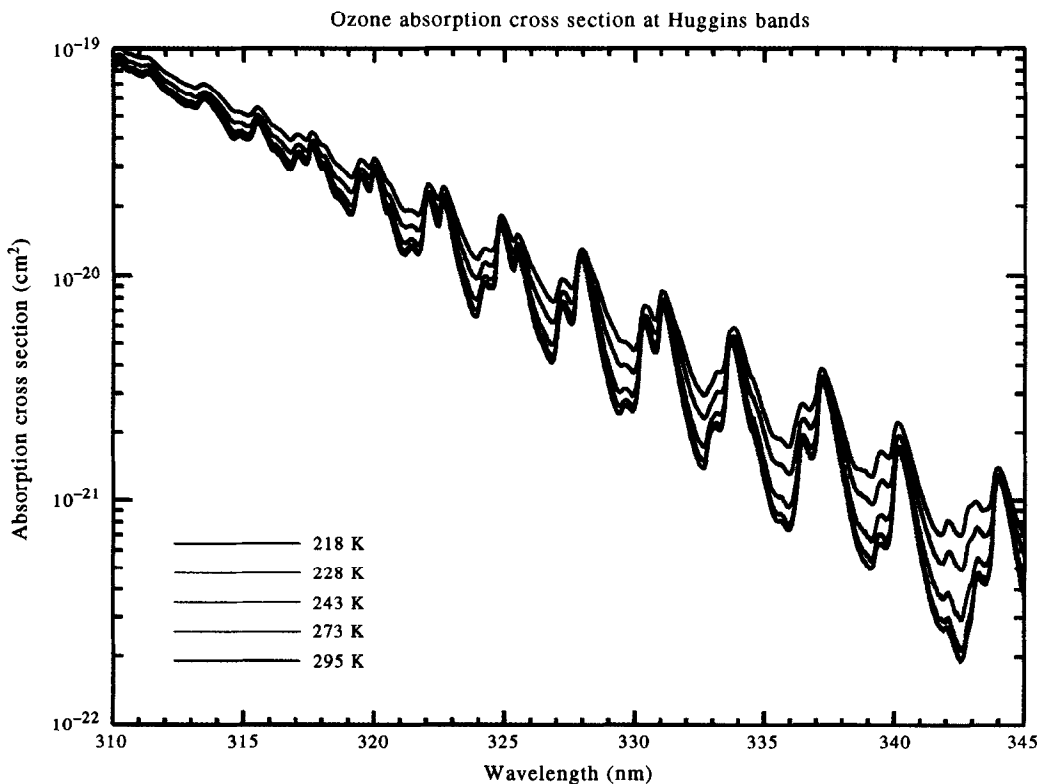


Fig. 1. Ozone absorption cross section of the Huggins bands in five different temperatures (218, 228, 243, 273 and 295 K).

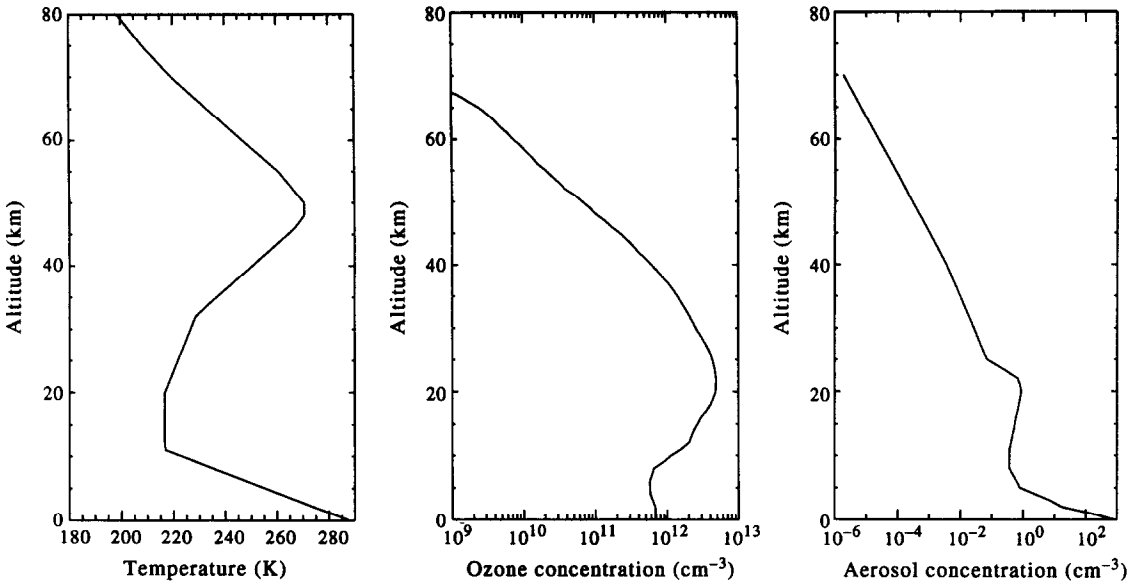


Fig. 2. Vertical profile of standard temperature, ozone and aerosol number density in the atmosphere.

less than 318 nm, the effect of ozone on the absorption spectrum is comparable to the other effects such as Rayleigh and aerosol scattering. The typical total optical depth is around 1.5 and gives rise to considerable scattering and absorption in the troposphere in this wavelength range. At longer wavelengths, the absorption due to ozone is less important.

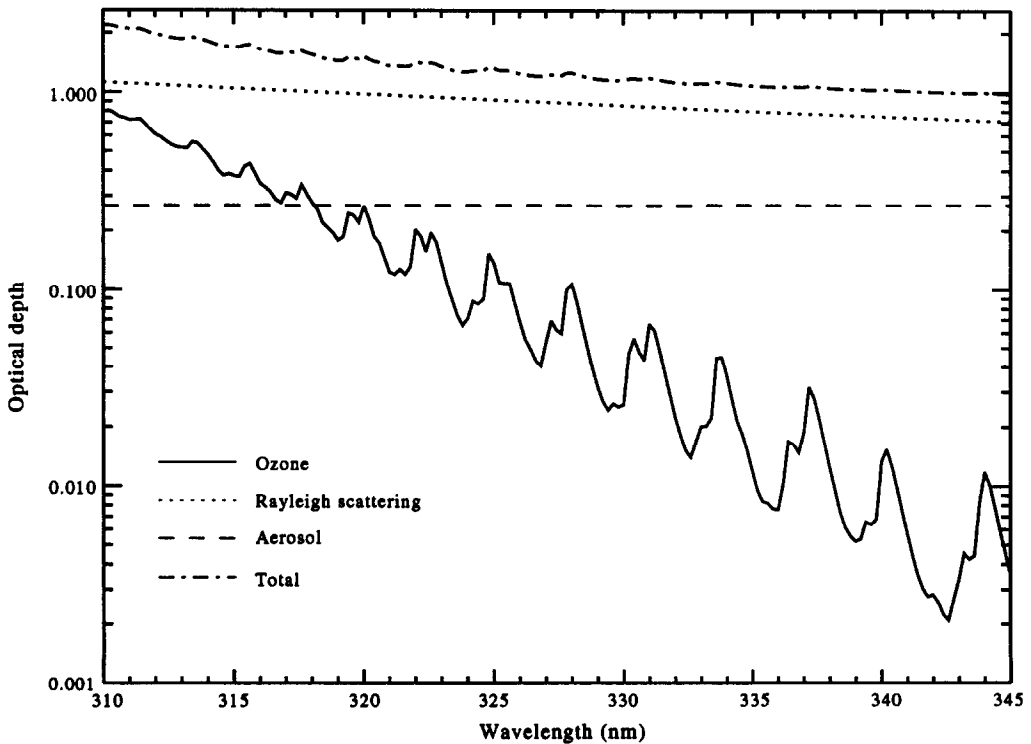


Fig. 3. Optical depth of ozone, Rayleigh scattering and aerosol in the Huggins bands. Due to the decreasing cross section as wavelength increases, ozone optical depth is much smaller than all the others in longer wavelength.

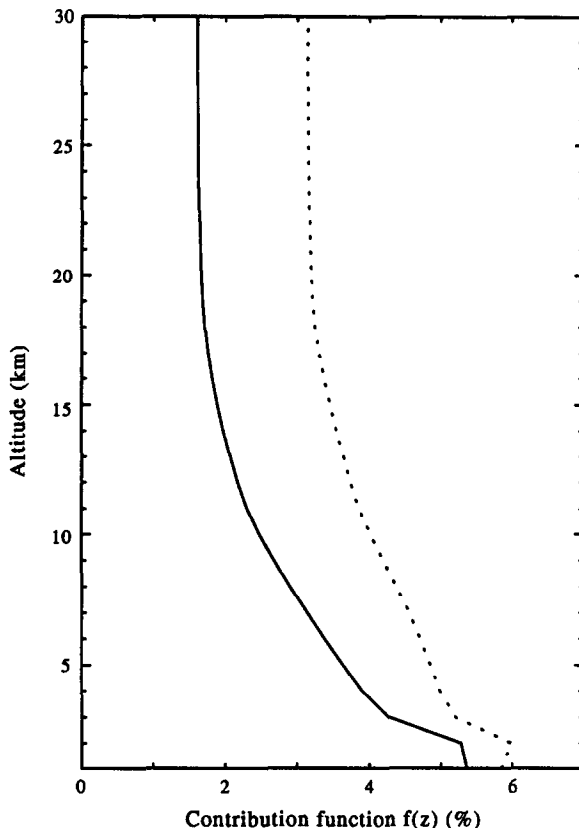


Fig. 4. Contribution function of diffuse irradiance at wavelength 313.47 nm at SZA 0° (—) and 60° (.....).

3. SENSITIVITY STUDY OF STRATOSPHERIC AND TROPOSPHERIC OZONE CHANGE

In this paper, we will study the transmission of the atmosphere in the Huggins bands using a ground-based measurement. The reference case is defined as a standard ozone profile in the radiative transfer model. In the following study, the azimuth angle is set to 0°.

Solar radiation is both absorbed and scattered in the atmosphere. Single scattering dominates in the middle atmosphere, while multiple scattering becomes important in the troposphere due to the higher concentration of air molecules and aerosols. Therefore, the diffuse solar radiation is greatly enhanced in the troposphere.^{10,11} In this section, we will apply this principle to the study of solar radiation transfer in the Huggins bands and show the possibility of detecting tropospheric ozone with high accuracy although it is much smaller compared to stratospheric ozone.

First, we will study the sensitivity of diffuse irradiance to tropospheric and stratospheric ozone changes relative to the reference case at different solar zenith angle (SZA) using contribution function $f_{\lambda, \theta_o}(z)$ of layer z which is defined as

$$f_{\lambda, \theta_o}(z) = \frac{I_{\lambda, \theta_o}(O_3(z) + 5DU) - I_{\lambda, \theta_o}(O_3(z))}{I_{\lambda, \theta_o}(O_3(z))}$$

where $O_3(z)$ is ozone vertical profile and $I_{\lambda, \theta_o}(O_3(z))$ is the reference diffuse irradiance at wavelength λ and solar zenith angle θ_o , $I_{\lambda, \theta_o}(O_3(z) + 5DU)$ is the diffuse irradiance when ozone in layer z is increased by 5DU. Figure 4 shows the contribution function for 313.47 nm at SZA 0 and 60°, respectively. As shown in Fig. 4, the contribution function is relatively constant in the stratosphere, but it increases in the troposphere due to an increase in multiple scattering. The averaged contribution function of the diffuse irradiance in the troposphere is about 1.5 times that of the stratosphere. The change of the SZA (from 0 to 60°) does not significantly change the relative contribution function between troposphere and stratosphere.

Let DIF be the diffuse irradiance specific intensity ($W\ nm^{-1}m^{-2}sr^{-1}$) and DIR be the direct solar irradiance ($W\ nm^{-1}m^{-2}$). Figure 5(a) shows the ratio DIF/DIR at three viewing angles (relative to

zenith) in reference case (solid lines) and in perturbed case (dotted lines) when $SZA = 0$. The increase of this ratio at shorter wavelength is due to the greater attenuation of the direct solar beam (DIR). The DIF also decreases at shorter wavelengths, but not as much as DIR. The Huggins bands of ozone are clearly seen in this figure. In the perturbed case tropospheric ozone is decreased in each level proportionally, with total decrease of 10 DU. The dotted lines show this new DIF/DIR ratio.

Figure 5(b) presents the relative change of the perturbed case (tropospheric ozone decreased by 10 DU) as compared to the reference case in the DIF/DIR ratio. Note that the changes become larger at the greater viewing angles. The same case is repeated for the decrease of stratospheric ozone by 10 DU. The difference, as shown by the dotted lines in Fig. 5(b), is very small in the stratospheric case and it remains constant as the viewing angle changes.

The distinction between changing the tropospheric versus the stratospheric ozone can be even more easily seen if we consider the difference in the DIF/DIR ratio as a function of viewing angle at a certain wavelength (312 nm here) (Fig. 6). Again in each perturbed case 10 DU of ozone has been taken out from the troposphere or the stratosphere. We obtain a characteristic profile with a peak at viewing angle around 85° depending on SZA for decreasing tropospheric ozone, while we get a constant value for decreasing stratospheric ozone. The physical reason is as follows. Ozone in the stratosphere contributes to both DIR and DIF only in single scattering. Therefore, the ratio DIF/DIR is independent of viewing angles (as long as we use the same SZA for observing DIF and DIR). tropospheric ozone contributes to DIR in single scattering, but contributes to DIF in multiple scattering. Since the latter changes with viewing angle, we get a large difference in the DIF/DIR ratio. In these characteristic profiles, we have a way to discriminate between tropospheric and stratospheric ozone. This will constitute the basis for our proposed experiment to measure tropospheric ozone.

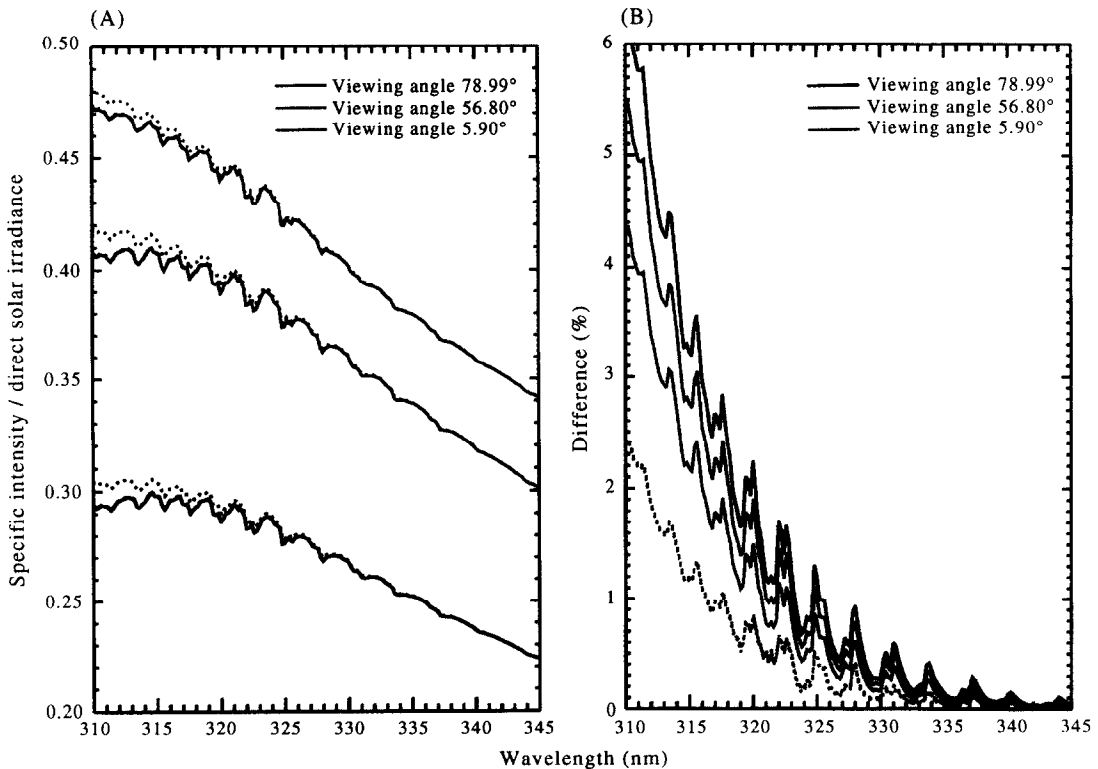


Fig. 5. (a) Ratio of specific intensity and direct solar irradiance in three viewing angles (5.90, 56.80, and 78.99) at SZA 0 with 0 azimuth angle. (—) and (.....) represent the reference and perturbed case, respectively. (b) Percent difference of the ratio relative to the reference state when either troposphere (-) or stratosphere (.....) is perturbed.

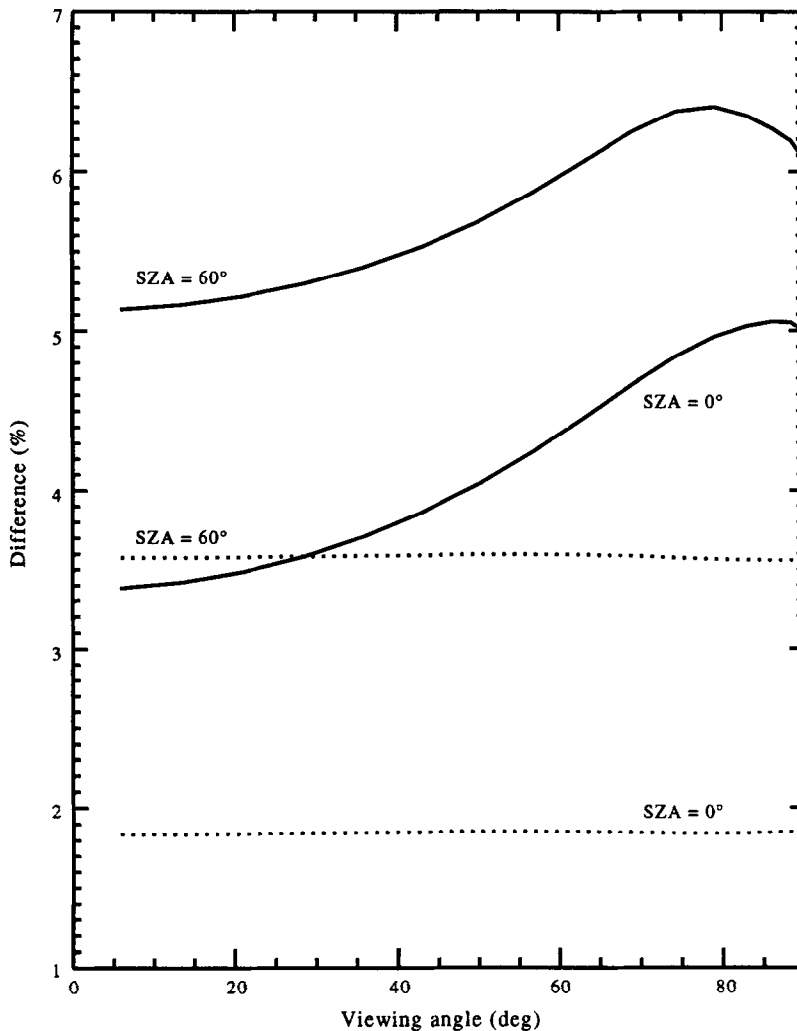


Fig. 6. Percent difference of the ratio at 312 nm as a function of viewing angle at SZA 0 and 60 when either troposphere (—) or stratosphere (.....) is perturbed.

4. THE RETRIEVAL ALGORITHM

In the last section we have provided a convincing demonstration that with appropriate measurements and modeling there is a sensitive way to distinguish between stratospheric and tropospheric ozone. The retrieval algorithm is based on this line of reasoning. In the absence of real data, we will develop a simple two parameter retrieval scheme. With the acquisition of observed data, we expect to further develop and improve this retrieval scheme.

We shall first make the simple assumption that atmospheric ozone profile $O_3(z)$ may be described as the superposition of two "typical" profiles,

$$O_3(z) = aS_{\text{ref}}(z) + bT_{\text{ref}}(z)$$

where $S_{\text{ref}}(z)$ is the reference vertical ozone profile for stratospheric ozone, and $T_{\text{ref}}(z)$ that for tropospheric ozone. The constants a and b are equal to unity for the 1976 U.S. Standard Atmosphere. In the retrieval algorithm, we will let a and b be undetermined parameters that will be chosen by minimizing the least square error between the model predictions of the observations computed using $O_3(z)$ and the actual observations. An example of the retrieval is given in Figs. 7 and 8. Figure 7 gives the "synthetic data" (solid line), with artificial "noise" (dash line) added. The "synthetic data" corresponds to $a = 0.934$, $b = 0.729$ at SZA 60°. Figure 8 shows the quality of the "fits" to the "synthetic data" with various sets of values for the parameters a and b . As expected, we get the minimum least square error at $a = 0.934 \pm 0.016$, $b = 0.729 \pm 0.136$. This very

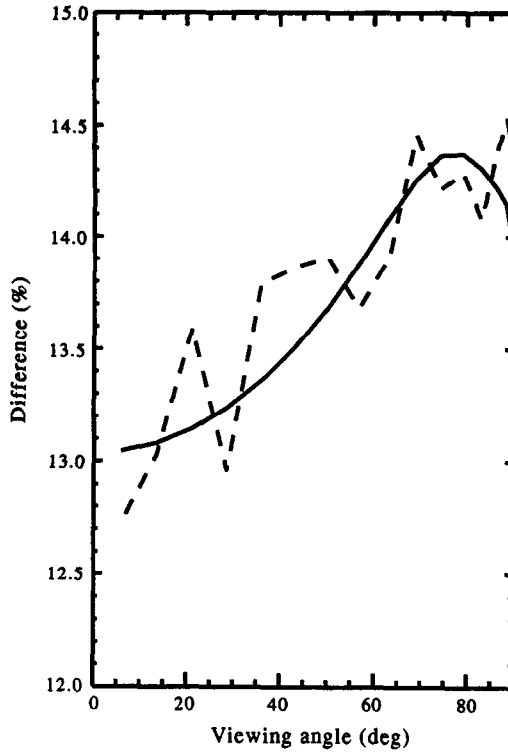


Fig. 7. Synthetic data (—) with artificial “noise” (---) added. The synthetic data corresponds to $a = 0.934$, $b = 0.729$ at SZA 60° .

crude retrieval scheme will be used as a first order solution to determine the tropospheric ozone column. As the data become available, we will be exploring new ways to improve upon this scheme so that we can extract more information on the vertical distribution of ozone in the atmosphere by studying the ozone Huggins bands transmission.

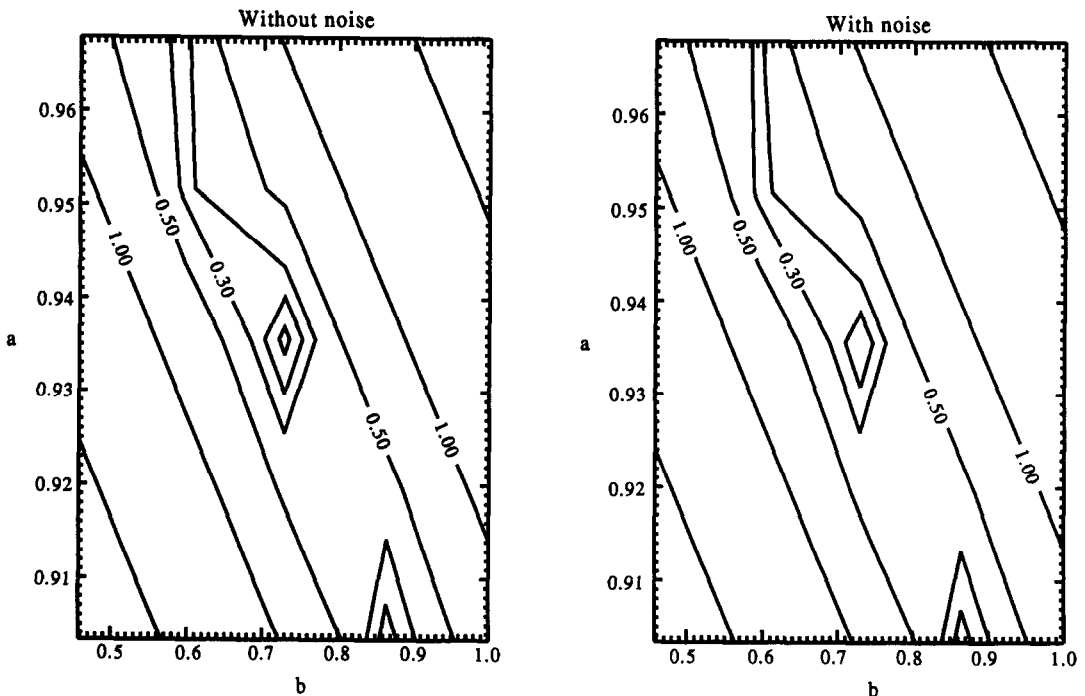


Fig. 8. Contour plots of the least square error (percentage difference) with and without noise added.

Since the difference between single scattering (e.g., in the stratosphere) and multiple scattering (e.g., troposphere) is essential for discriminating stratospheric and tropospheric ozone, we believe that another useful discriminant may be the polarization of the diffuse light. Single scattering of u.v. radiation by air molecules is strongly polarized. On the other hand, multiple scattering tends to randomize polarization. This may provide another powerful constraint on the origin of the diffuse radiation (whether it is from the stratosphere or troposphere).

In this study, we have not considered the Ring effect.¹² But our method is not sensitive to this effect, and we can always choose wavelengths at which the Ring effect is minimal.

5. CONCLUSIONS

This paper presents the preliminary results of a novel technique to measure tropospheric ozone by remote sensing from the ground. It provides the theoretical background for future measurement and retrieval of tropospheric ozone. The principal findings in this paper are summarized as follows:

1. due to the multiple scattering of air molecules and aerosols, the signal due to absorption of tropospheric ozone is amplified by as much as 1.5 times compared to that of the stratosphere in the Huggins bands;
2. the characteristic profile (Fig. 6) related to the tropospheric ozone change is found and this enables us to separate the tropospheric from stratospheric ozone in the transmitted spectrum measurements. The influence of profile shapes for stratospheric and, especially, tropospheric ozone will influence the derived tropospheric column ozone and must be considered in more detail;
3. a simple retrieval algorithm is demonstrated to effectively obtain the tropospheric column ozone.

Acknowledgements—We thank R. S. Stolarski, R. Cageao, M. Allen, R. McPeters, M. Newchurch, and J.-H. Kim for valuable comments. This work was supported by National Science Foundation grant ATM 9526209 and NASA grant NAG1-1806 to the California Institute of Technology. Contribution number 5674 from the Division of Geological and Planetary Sciences, California Institute of Technology. After this work was completed, it was pointed out to us by R. McPeters that similar ideas were proposed by Green et al.¹³

REFERENCES

1. J. A. Logan, M. J. Prather, S. C. Wofsy and M. B. McElroy, *J. Geophys. Res.* **86**, 7210 (1981).
2. J. A. Logan, *J. Geophys. Res.* **99**, 25553 (1994).
3. J. Fishman, C. E. Watson, J. C. Larsen and J. A. Logan, *J. Geophys. Res.* **95**, 3599 (1990).
4. Y. Jiang and Y. L. Yung, *Science* **272**, 714 (1996).
5. S. P. Sander, R. P. Cageao and R. R. Friedl, *S.P.I.E. Proceedings Series* **1715**, 15 (1993).
6. J. Malicet, D. Daumont, J. Charbonnier, C. Parisse, A. Chakir and J. Brion, *J. Atmos. Chem.* **21**, 263 (1995).
7. D. V. Michelangeli, M. Allen, Y. L. Yung, R. L. Shia and D. Crisp, *J. Geophys. Res.* **97**, 865 (1992).
8. K. L. Demerjian, K. L. Schere and J. T. Peterson, *Adv. Environ. Sci. Tech.* **10**, 369 (1980).
9. T. F. Eck, P. K. Bhartia, P. H. Hwang and L. L. Stowe, *J. Geophys. Res.* **92**, 4287 (1987).
10. C. Bruhl and P. J. Crutzen, *Geophys. Res. Lett.* **16**, 703 (1989).
11. K. Stamnes, *Surveys in Geophysics* **14**, 167 (1993).
12. J. Joiner, P. K. Bhartia, R. P. Cebula, E. Hilsenrath, R. D. McPeters and H. Park, *Appl. Opt.* **34**, 4513 (1995).
13. A. E. S. Green and K. F. Klenk, *Technical Proceedings of the First International Interactive Workshop on Inversion Methods in Atmospheric Remote Sounding*, p. 297 (1977).